

Figure 1: Diagram showing the assumption of most lake depth models that the nearshore slope is extends into the lake and that all lakes have a common relationship between nearshore and in-lake slope.

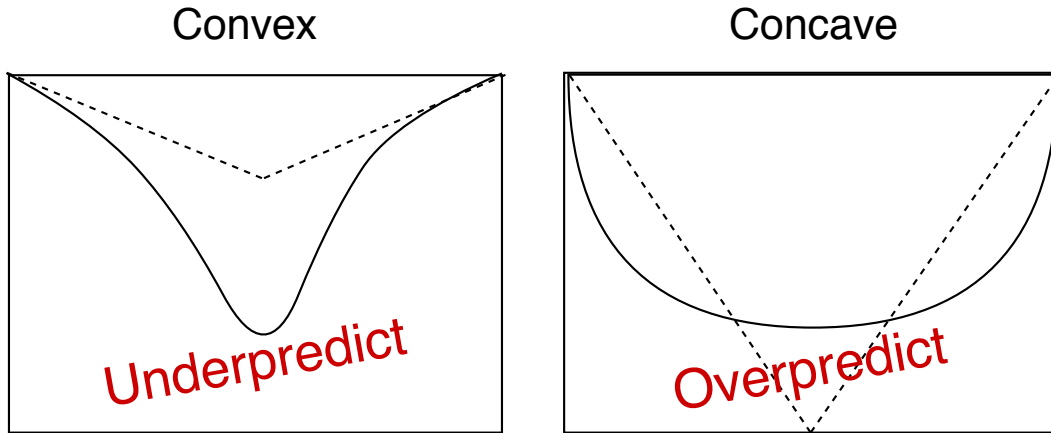


Figure 2: Diagram showing our expectation that slope-based models of lake depth will under predict true depth in convex lakes (left) and over predict true depth in concave lakes (right)

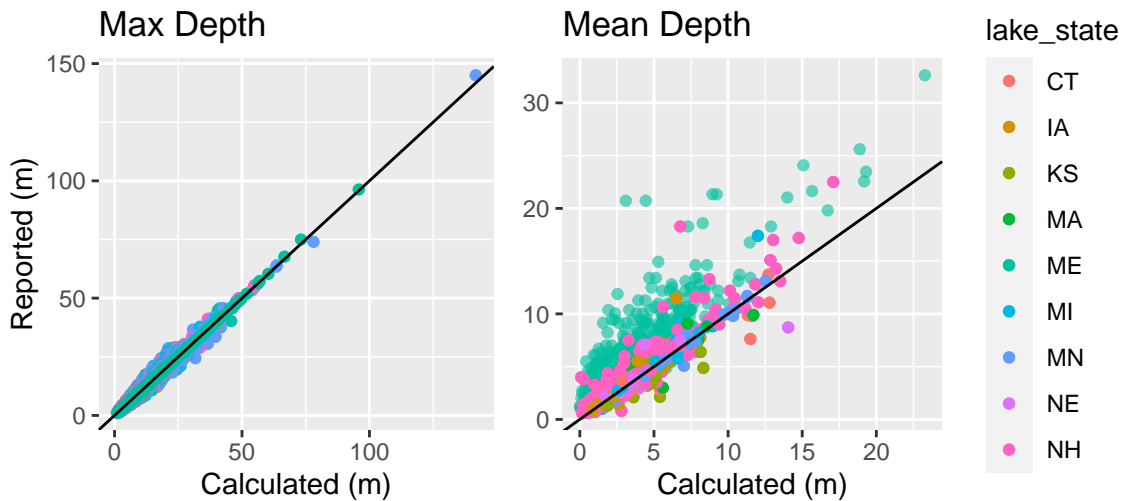


Figure 3: Comparison between reported max depth and max depth calculated from bathymetry surfaces.

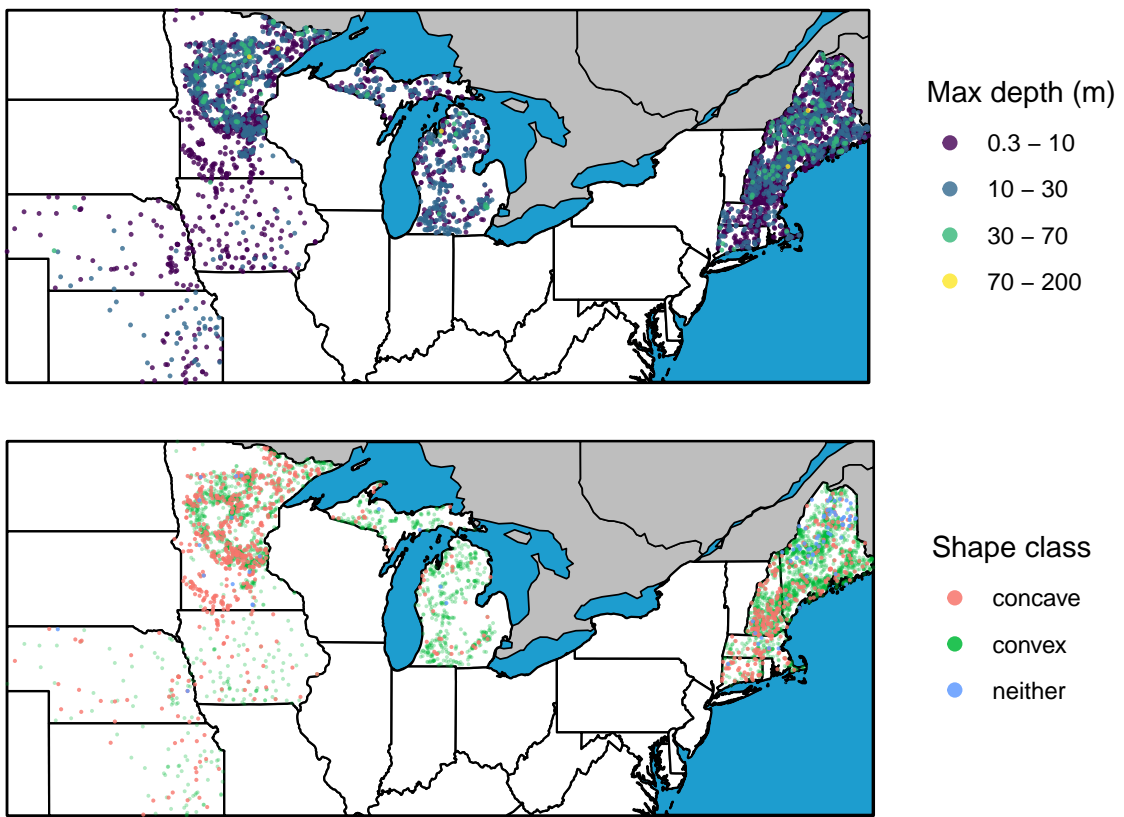


Figure 4: Map of lake maximum depth measurements calculated from lake bathymetry surfaces.

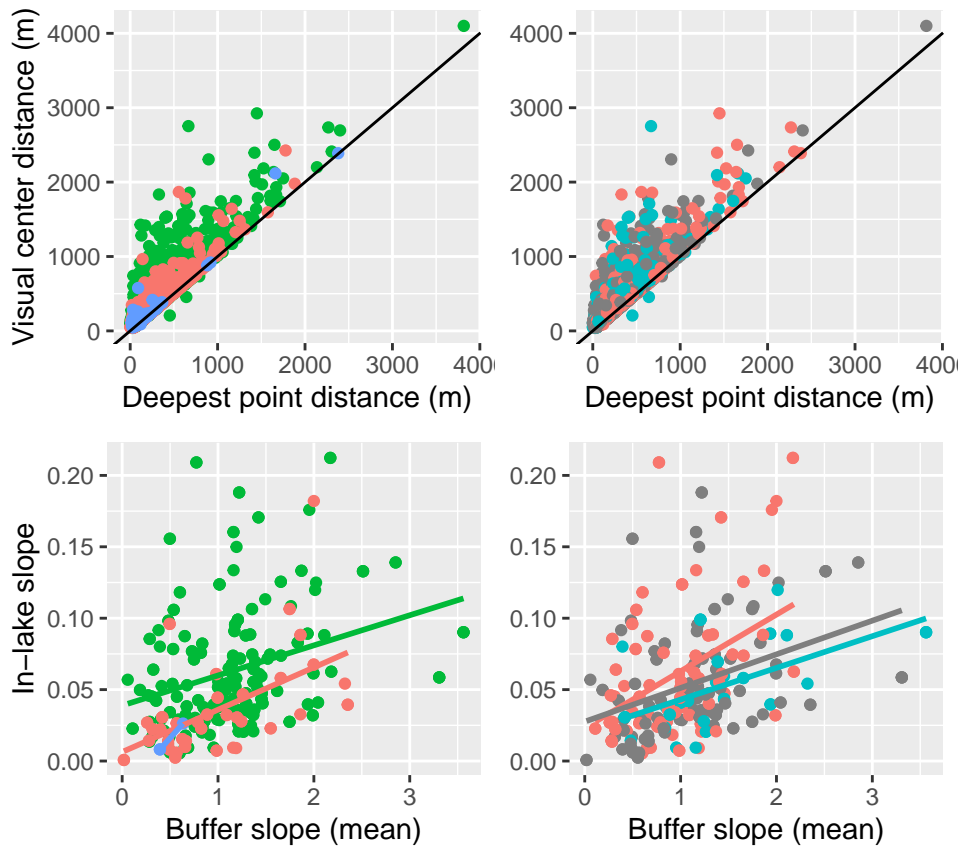


Figure 5: Comparison among lake shape and reservoir classes for A-B) distance to deepest point versus distance to lake visual center and C-D) buffer slope versus inlake slope.

variable	Median	Q25	Q75	n
lake_maxdepth_m	7	3.7	12	17700
lake_meandepth_m	3	1.7	4.8	8020
has_limno	1	1	1	17700
shape_offset	-17	-30	-4	4990
lake_elevation_m	340	210	460	17700
lake_waterarea_ha	33	11	100	17700
lake_totalarea_ha	33	11	100	17700
lake_islandarea_ha	0	0	0.076	17700
lake_perimeter_m	3500	1800	7300	17700
lake_islandperimeter_m	0	0	120	17700
lake_shorelinedevfactor_nounits	1.7	1.4	2.2	17700
nws_focallakewaterarea_ha	100	37	390	5190
nws_area_ha	5100	1500	29000	5190
nws_lake_arearatio	48	17	190	5190
nws_perimeter_m	75000	38000	2e+05	5190
nws_mbgonhull_width_m	7600	4100	17000	5190
nws_meanwidth_m	3900	2100	9000	5190
nws_mbgonhull_length_m	13000	7100	32000	5190
nws_mbgonhull_orientation_deg	95	47	140	5190
ws_focallakewaterarea_ha	33	11	100	17700
ws_area_ha	360	120	1400	17700
ws_lake_arearatio	10	4.4	28	17700
ws_perimeter_m	19000	9900	39000	17700
ws_mbgonhull_width_m	2100	1200	4100	17700
ws_meanwidth_m	1000	570	2100	17700
ws_mbgonhull_length_m	3600	2000	7000	17700
ws_mbgonhull_orientation_deg	90	42	140	17700
buffer100m_slope_max	20	15	27	12800
buffer100m_slope_mean	4.2	2.7	6.1	12800
dist_deepest	180	110	290	5020
dist_viscenter	240	150	390	5020
dist_between	140	44	390	5020
inlake_slope	0.046	0.024	0.079	5020

Figure 6: Summary of lake depth predictor variables.

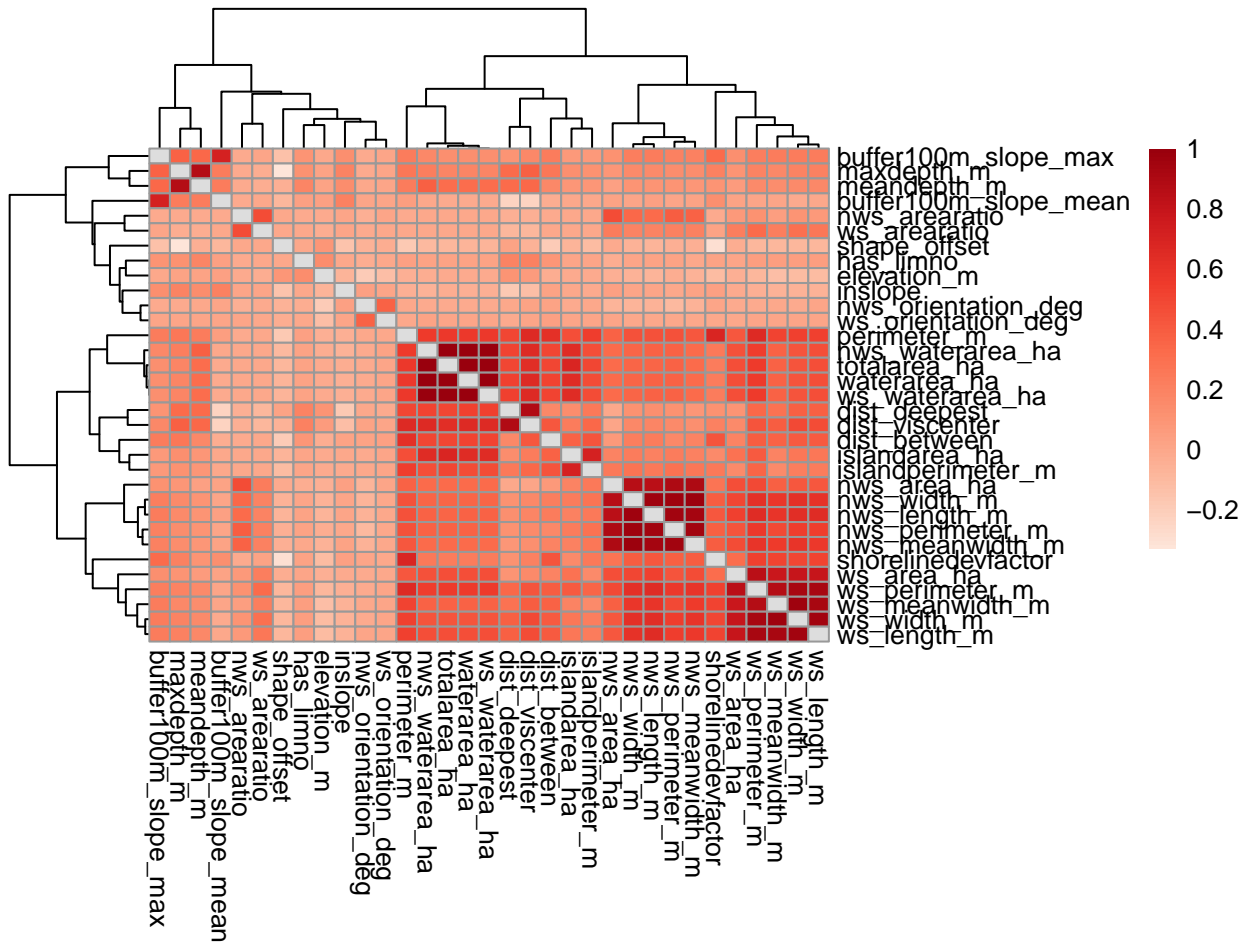


Figure 7: Correlation matrix heatmap.

### Normalized hypsography for 4994 lakes

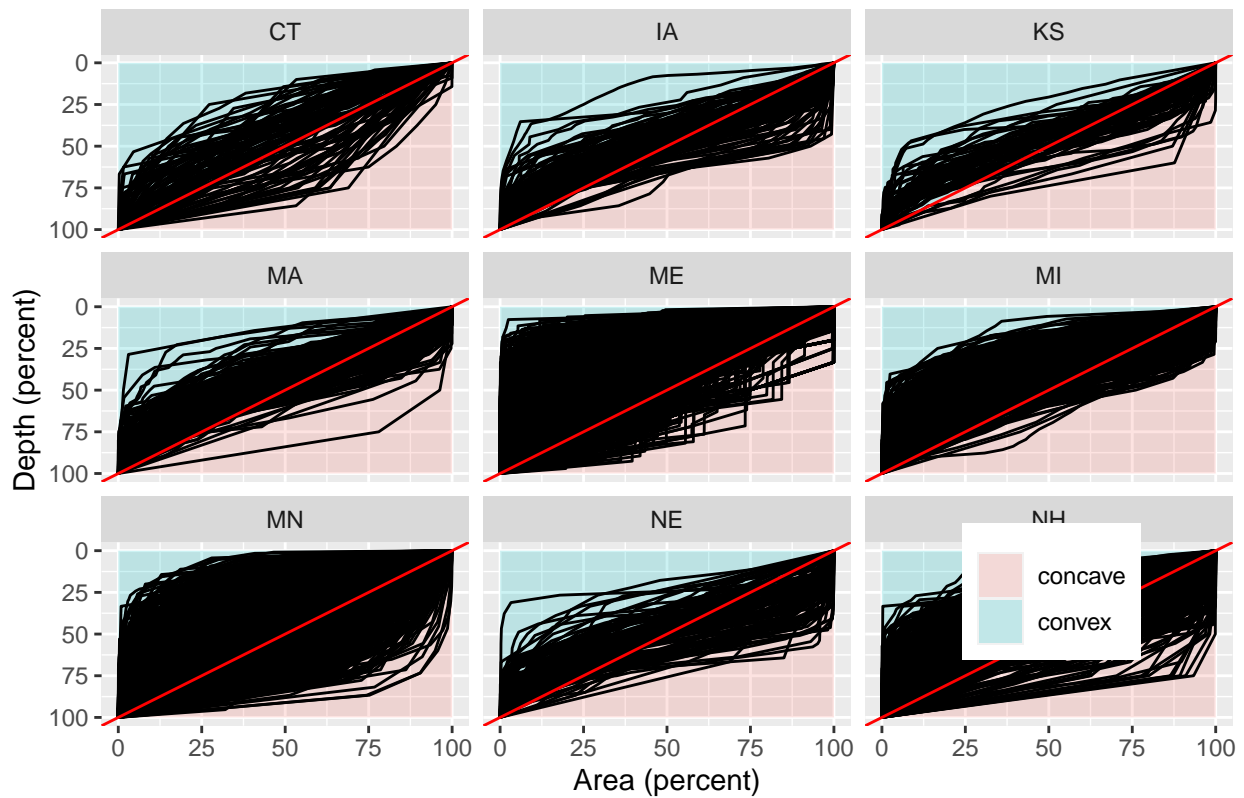


Figure 8: Hypsography classification by state.

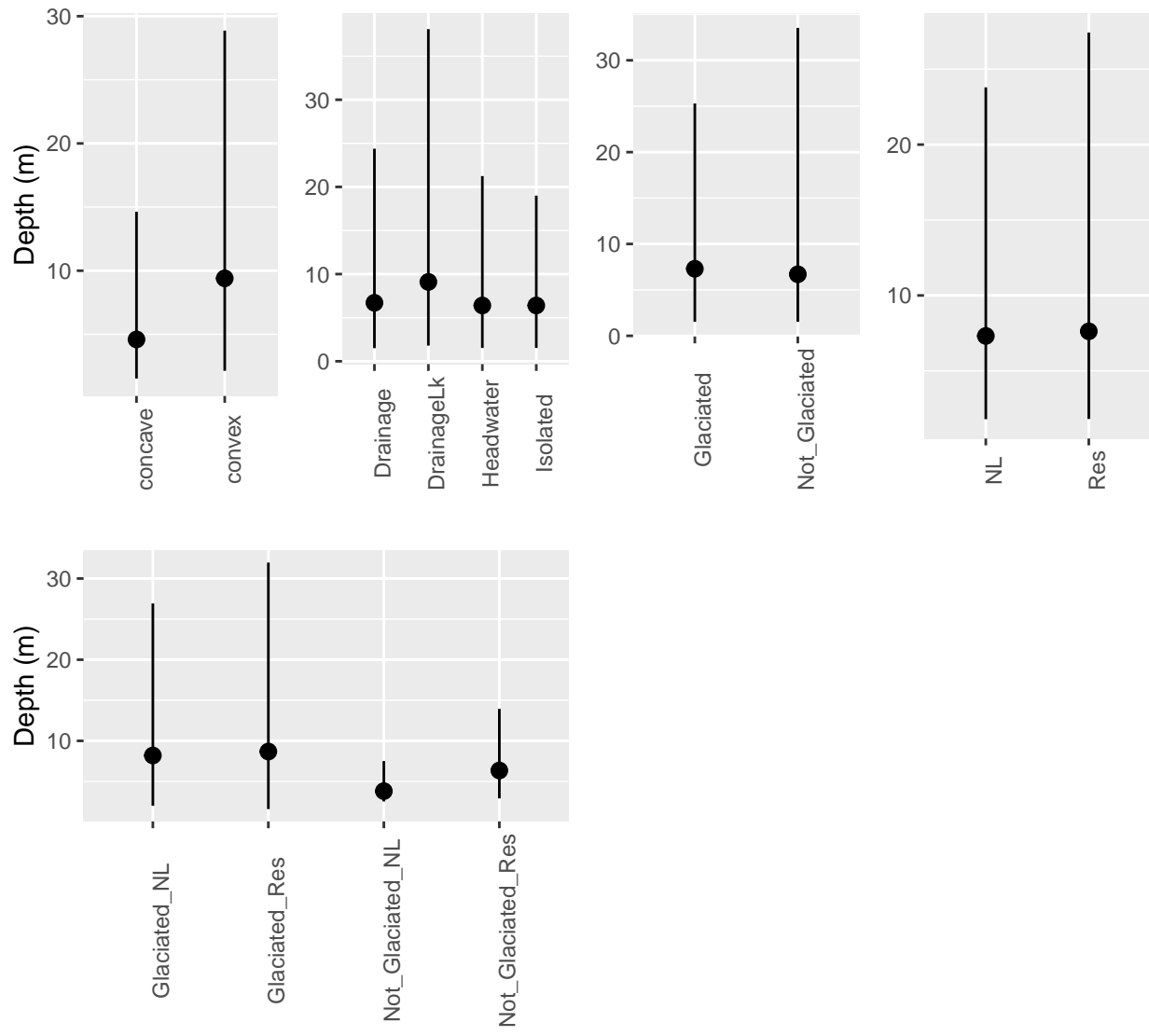


Figure 9: Lake maximum depth by categorical variables.

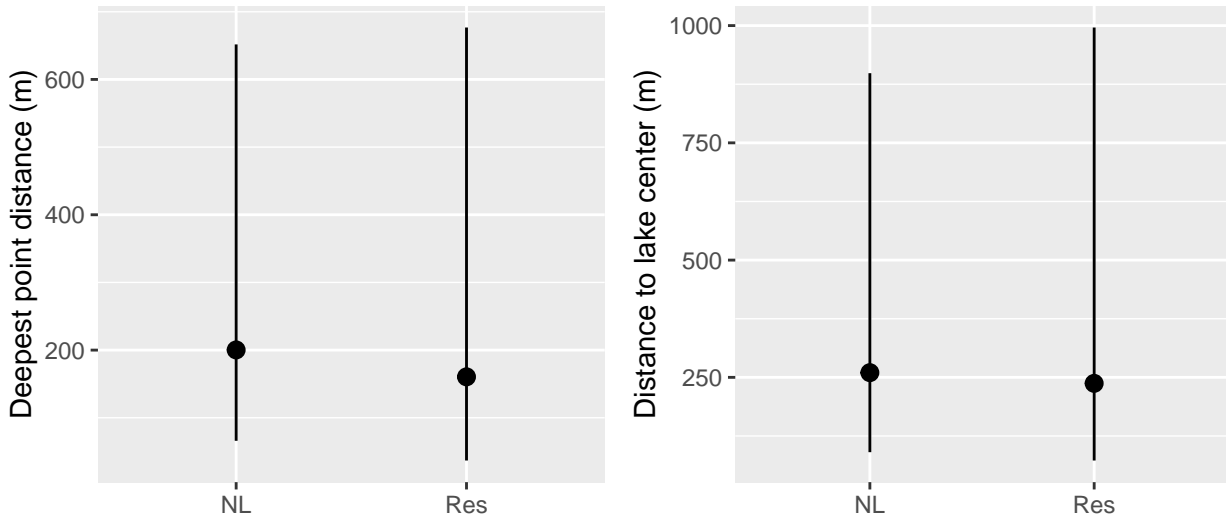


Figure 10: Contrasting distance from shore to the deepest point in the lake and distance to the lake visual center for natural lakes and reservoirs.

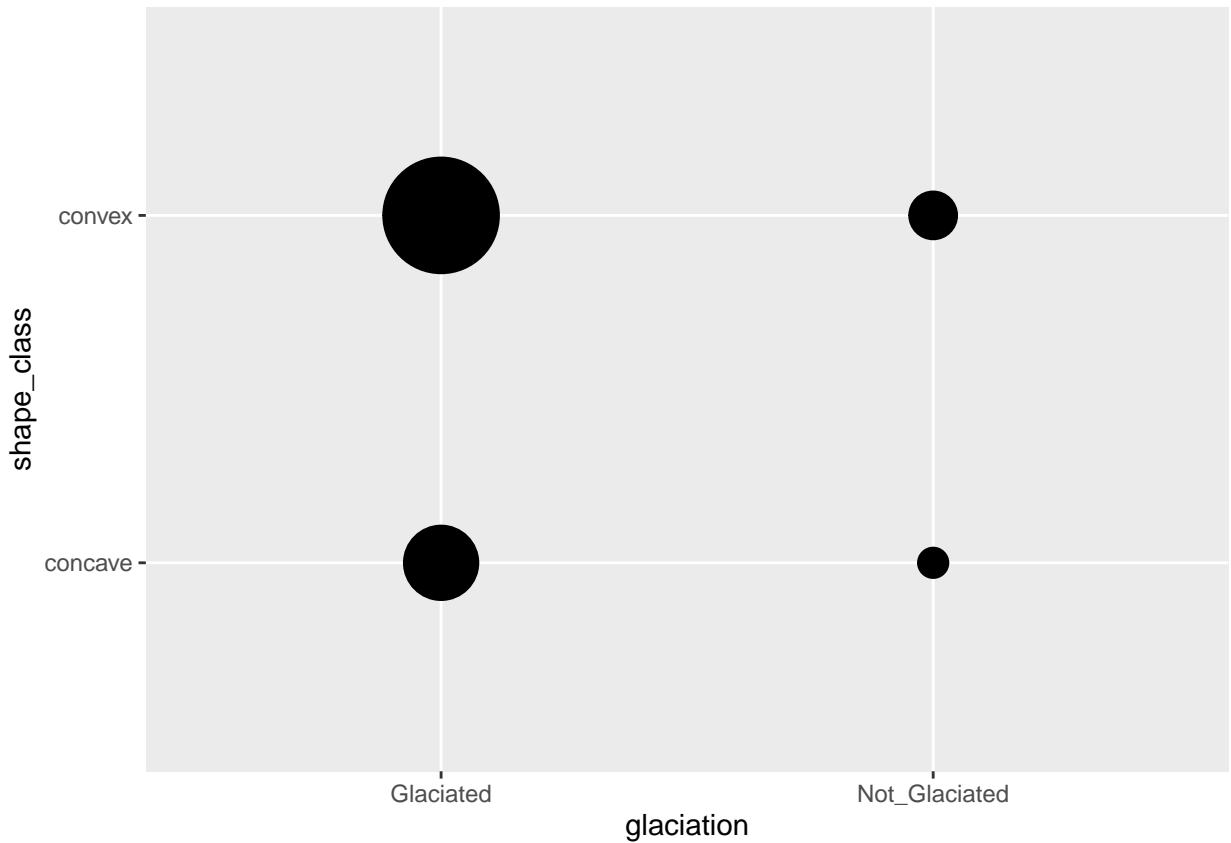


Figure 11: Cross tabulation between lake glaciation and shape class. Circles are proportional to the number of lakes in each category. If a lake has been glaciated it is more likely to be convex. However, if a lake has not been glaciated there is no tendency towards a particular shape class.

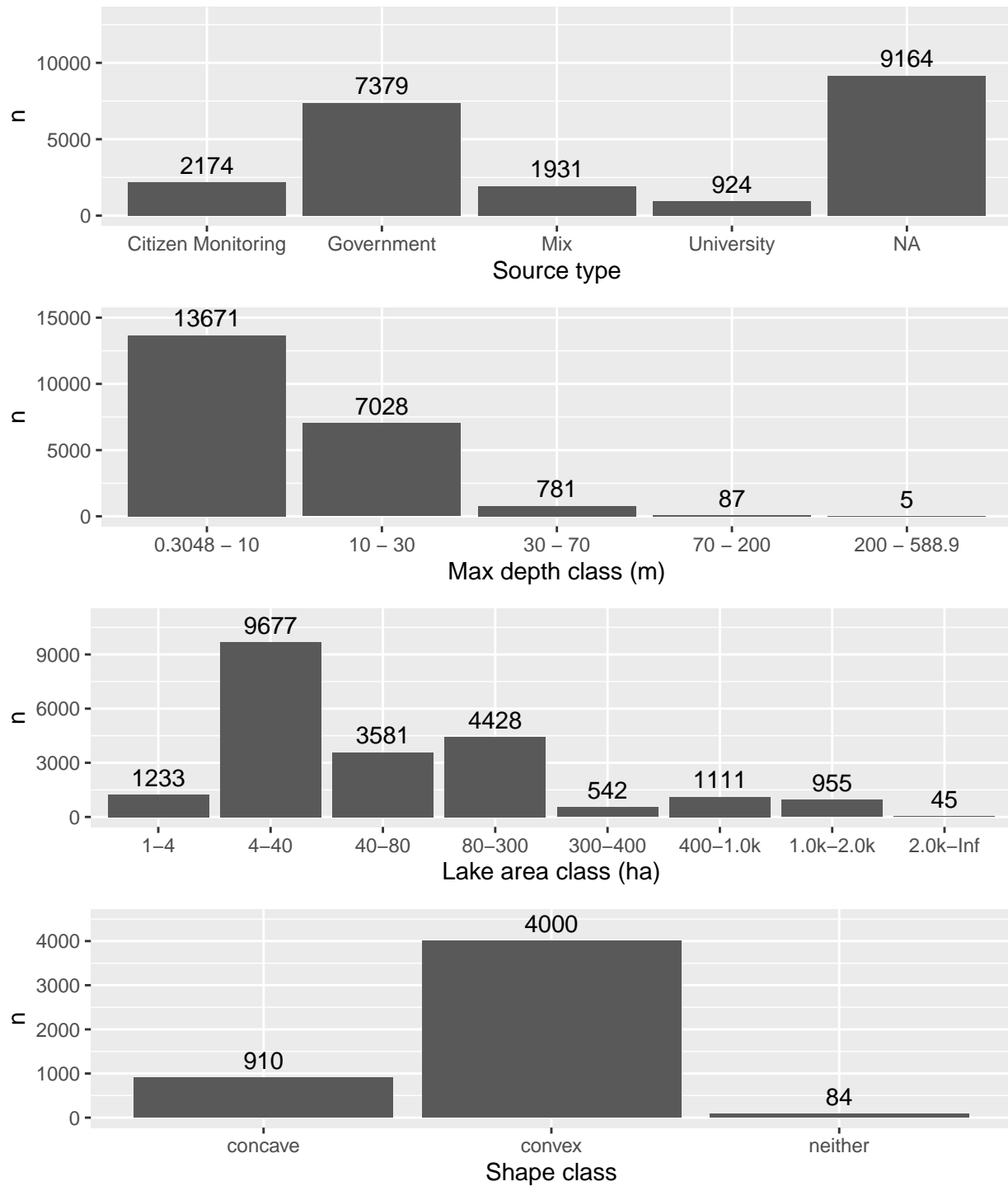


Figure 12: Number of lake depth measurements by categories.

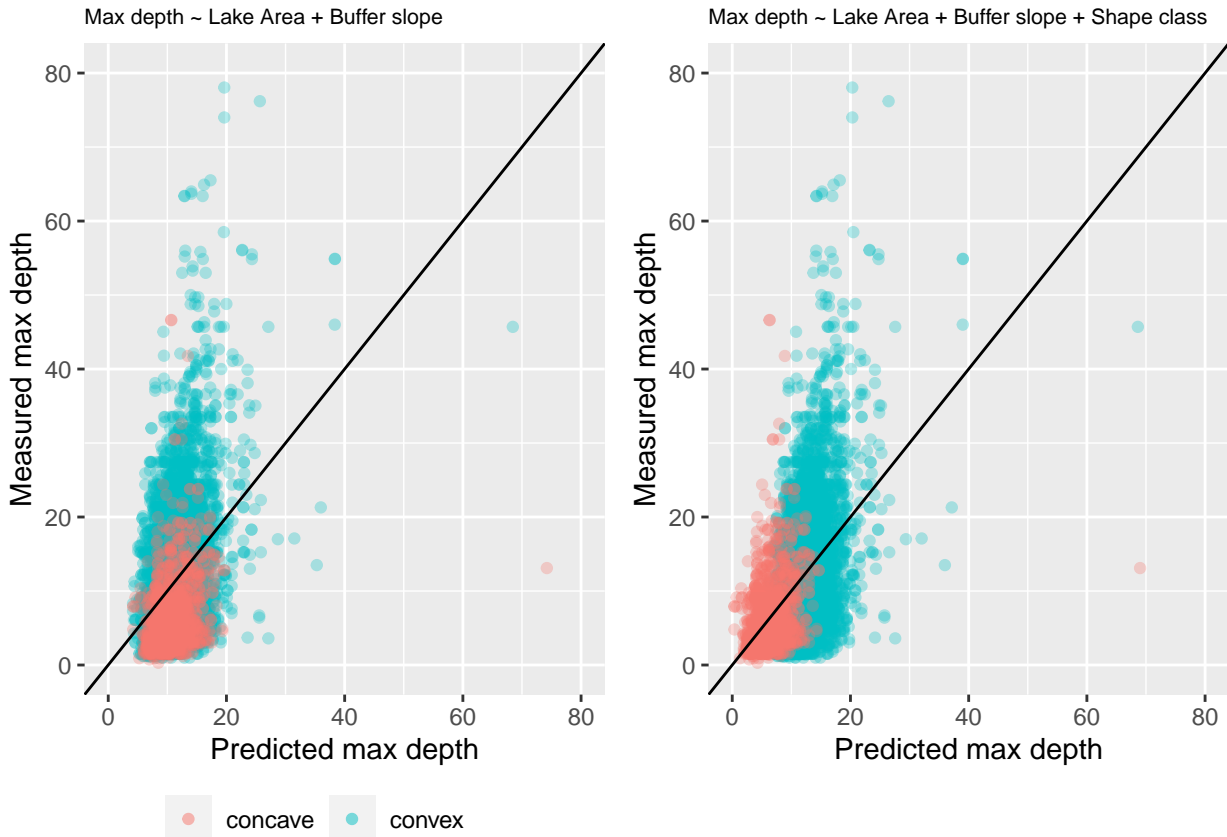


Figure 13: A model that does not include shape class over predicts depth in concave lakes but does not systematically under predict depth in convex lakes.

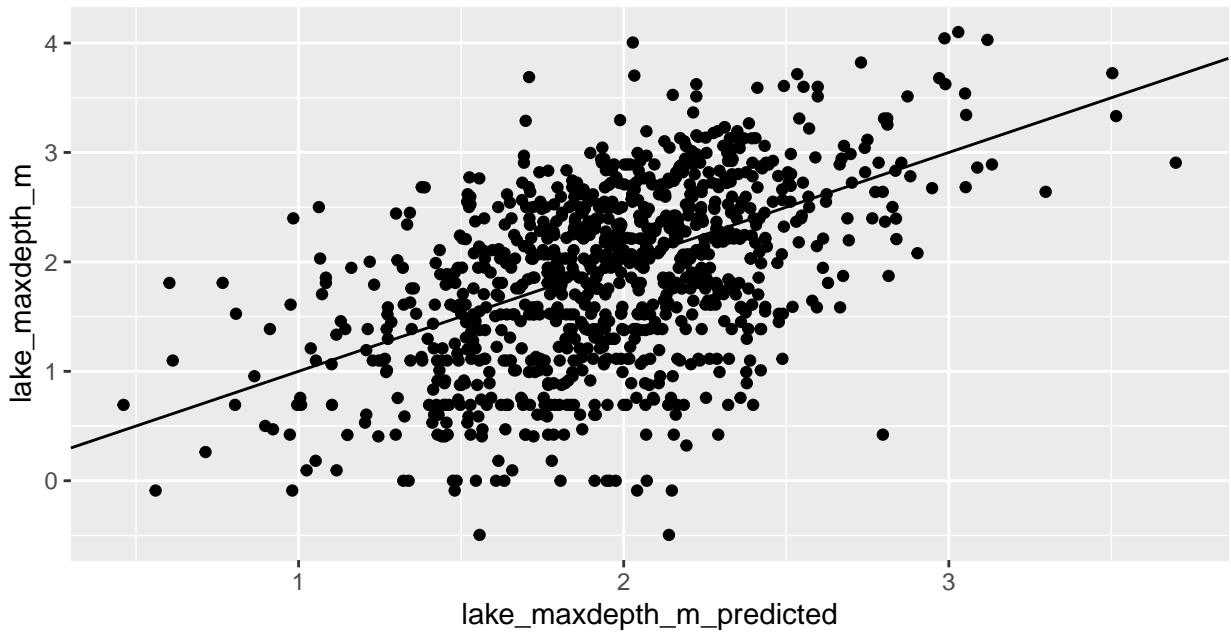


Figure 14: Reproduction of Oliver 2016 using LAGOSUS data in LAGOSNE footprint.

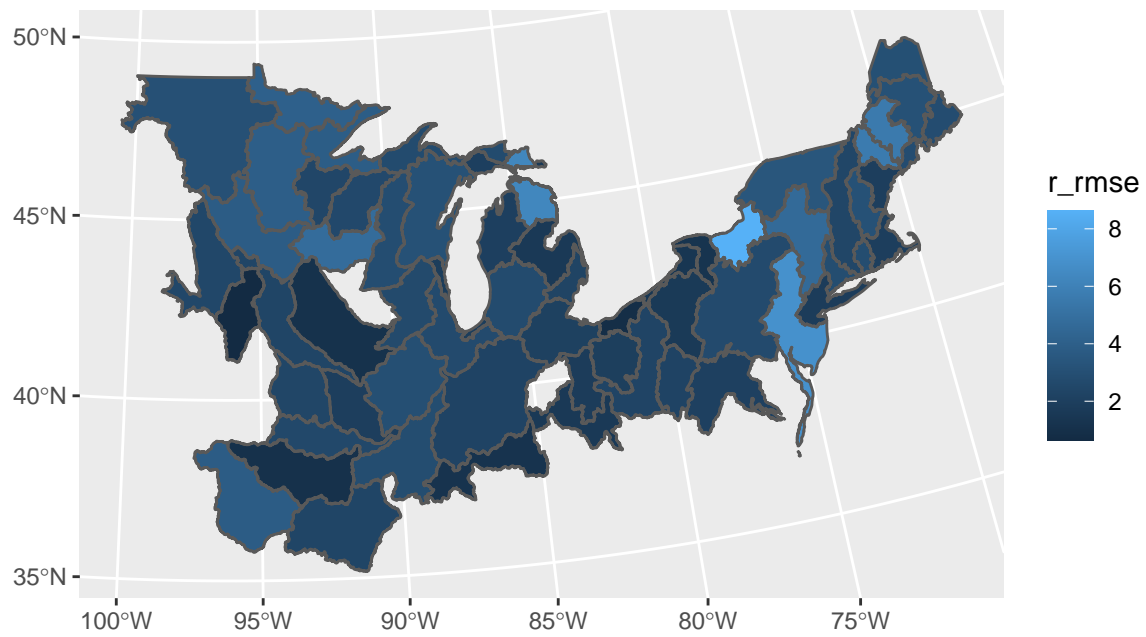


Figure 15: Reproduction of Oliver 2016 using LAGOSUS data in LAGOSNE footprint.

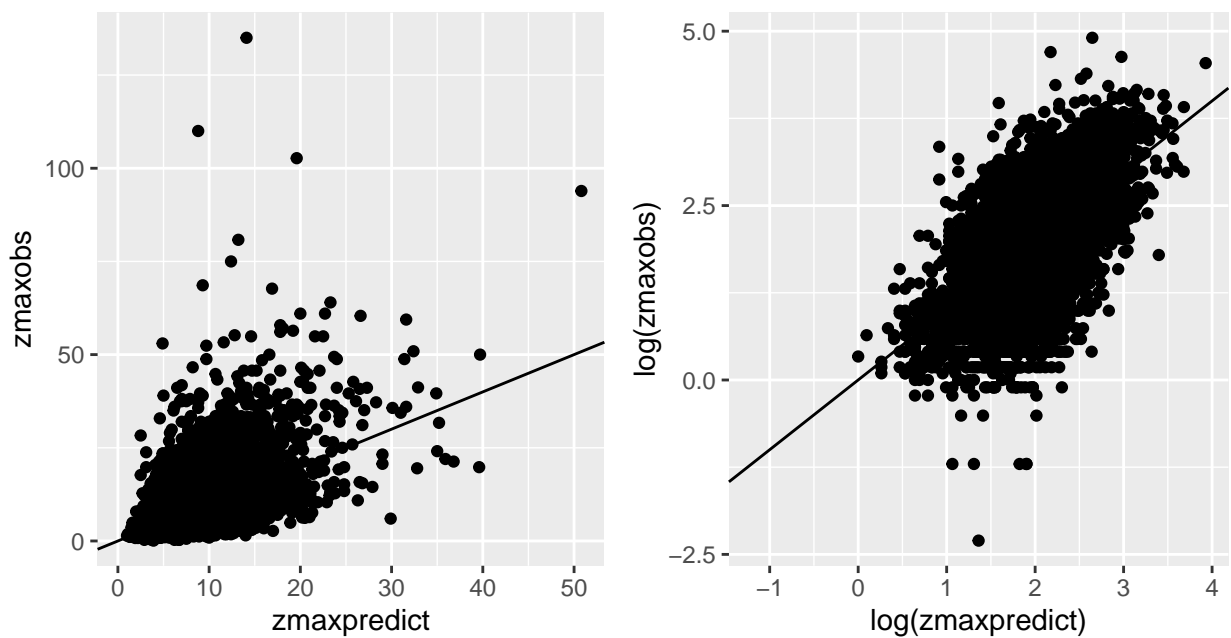


Figure 16: Oliver 2016 observed versus predicted.

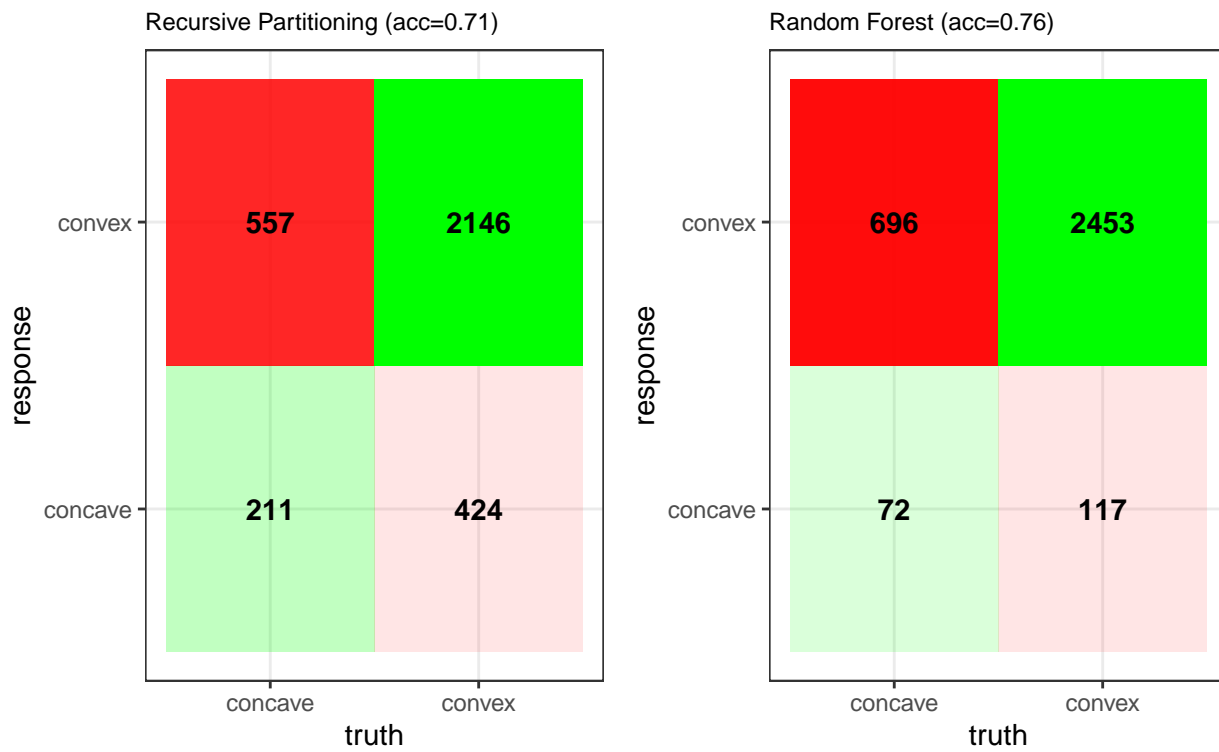


Figure 17: Confusion matrix comparing two classification methods

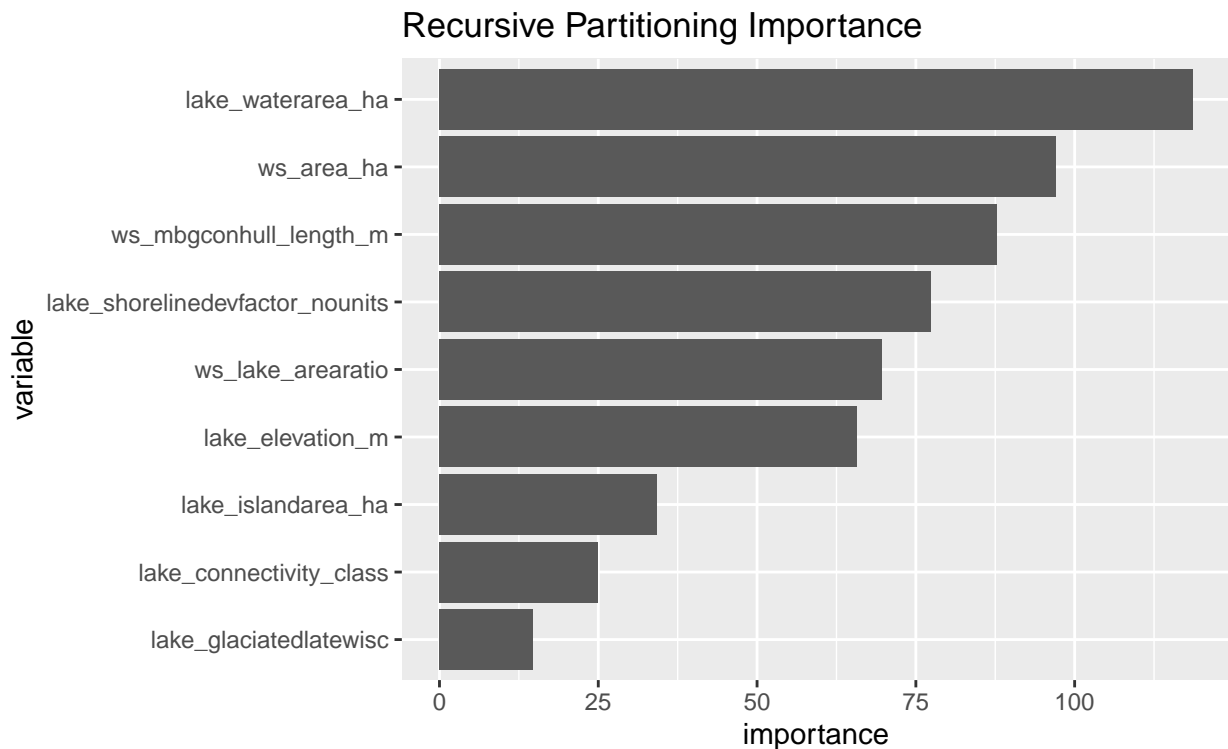


Figure 18: Recusive Partitioning variable importance.

**Supplementary Table 4. Equations of the six best-fit statistical models of increasing complexity tested in this study.**

Model	Size class by area [km <sup>2</sup> ]	Best-fit equation	Residual variance s <sup>2</sup>
1	All	$\log_{10}(D) = 0.6625 + 0.2289 \times \log_{10}(A)$	0.1150
2	All	$\log_{10}(D) = -0.0144 + 0.6887 \times \log_{10}(D_t)$	0.0765
3	All	$\log_{10}(D) = 0.0549 + 0.0774 \times \log_{10}(A) + 0.5893 \times \log_{10}(elv_{25\%})$	0.0790
4	All	n/a	n/a
	0.1-1	$\log_{10}(D) = 0.2045 + 0.0687 \times \log_{10}(A) + 0.4226 \times \log_{10}(elv_{25\%})$	0.0719
	1-10	$\log_{10}(D) = -0.0381 + 0.1315 \times \log_{10}(A) + 0.6488 \times \log_{10}(elv_{25\%})$	0.0814
	10-100	$\log_{10}(D) = -0.1535 - 0.0208 \times \log_{10}(A) + 0.8432 \times \log_{10}(elv_{25\%})$	0.0853
	100-500	$\log_{10}(D) = -0.3501 - 0.0024 \times \log_{10}(A) + 0.9216 \times \log_{10}(elv_{25\%})$	0.1044
5	All	n/a	n/a
	0.1-1	$\log_{10}(D) = 0.3826 + 0.1512 \times \log_{10}(A) + 0.4820 \times \log_{10}(S_{100})$	0.0678
	1-10	$\log_{10}(D) = 0.1801 + 0.2985 \times \log_{10}(A) + 0.8473 \times \log_{10}(S_{100})$	0.0689
	10-100	$\log_{10}(D) = 0.0379 + 0.2445 \times \log_{10}(A) + 1.1517 \times \log_{10}(S_{100})$	0.0692
	100-500	$\log_{10}(D) = 0.0123 + 0.2664 \times \log_{10}(A) + 1.1474 \times \log_{10}(S_{100})$	0.1094
6	All	n/a	n/a
	0.1-1	$\log_{10}(D) = 0.3346 + 0.1221 \times \log_{10}(A) + 0.3673 \times \log_{10}(S_{100}) + 0.1150 \times \log_{10}(D_t)$	0.0677
	1-10	$\log_{10}(D) = 0.0606 + 0.2158 \times \log_{10}(A) + 0.2808 \times \log_{10}(S_{100}) + 0.5771 \times \log_{10}(D_t)$	0.0678
	10-100	$\log_{10}(D) = -0.0692 + 0.0823 \times \log_{10}(A) + 0.7609 \times \log_{10}(S_{100}) + 0.4080 \times \log_{10}(D_t)$	0.0636
	100-500	$\log_{10}(D) = 0.0479 + 0.1260 \times \log_{10}(A) + 0.9462 \times \log_{10}(S_{100}) + 0.2350 \times \log_{10}(D_t)$	0.1071

D is the predicted mean depth in meters; A is the surface area of the lake in km<sup>2</sup>; D<sub>t</sub> is the topographic mean depth in meters; elv<sub>25%</sub> is the difference in meters between lake surface and mean landscape elevation within a buffer width equal to 25% of the diameter of a circle that represents the lake area; and S<sub>100</sub> is the average slope within a 100 m buffer around the lake in

Figure 19: Messager et al. 2016 equation table



Figure 20: Green points show the ‘visual center’ of the lake. Red points show the true deepest point of a lake.